J Nanopart Res (2016) 18:230
DOI 10.1007/s11051-016-3463-5

RESEARCH PAPER

Capping biological quantum dots with the peptide CLPFFD to increase stability and to reduce effects on cell viability

A. L. Riveros · J. Astudillo · C. C. Vásquez · Danilo H. Jara · Ariel R. Guerrero · F. Guzman · I. O. Osorio-Roman · M. J. Kogan

Received: 31 August 2015 / Accepted: 26 May 2016 / Published online: 11 August 2016

Abstract Highly fluorescent nanoparticles, or quantum dots, have multiple applications in biology and biomedicine; however, in most cases, it is necessary to functionalize them to enhance their biocompatibility and selectivity. Generally, functionalization is performed after nanoparticle synthesis and involves the use of molecules or macromolecules having two important traits: specific biological activity and functional groups that facilitate nanoparticle capping (i.e. atom–atom interaction). For this reason, we carried out a simple protocol for the chemical synthesis of cadmium telluride quantum dots capped with glutathione, and we then functionalized these nanoparticles with the amphipathic peptide CLPFFD. This peptide attaches selectively to β-Amyloid fibres, which are involved in Alzheimer's disease. Our results show that the optical properties of the quantum dots are not affected by functionalization with this peptide. Infrared spectra showed that cadmium telluride quantum dots were functionalized with the peptide CLPFFD. In addition, no significant differences were observed between the surface charge of the quantum dots with or without CLPFFD and the nanocrystal size calculated for HR-TEM was 4.2 nm. Finally, our results show that quantum dots with CLPFFD are stable and that they resulted in a significantly reduced cytotoxicity with respect to that induced by quantum

Electronic supplementary material The online version of this article (doi:10.1007/s11051-016-3463-5) contains supplementary material, which is available to authorized users.

A. L. Riveros (✉) · A. R. Guerrero · M. J. Kogan (✉)
Facultad de Ciencias Químicas y Farmacéuticas, Universidad de Chile, Santos Dumont No 964, Independencia, Casilla 233, Santiago, Chile
e-mail: ariveros@postqyf.uchile.cl

M. J. Kogan
e-mail: mkogan@ciq.uchile.cl

A. L. Riveros · A. R. Guerrero · M. J. Kogan
Advanced Center for Chronic Diseases, Santiago, Chile

J. Astudillo · C. C. Vásquez
Facultad de Química y Biología, Universidad de Santiago de Chile, Alameda 3363, Casilla 40, Santiago, Chile
e-mail: jason.astudillo@usach.cl

C. C. Vásquez
e-mail: claudio.vasquez@usach.cl

D. H. Jara
Radiation Laboratory, Department of Chemistry and Biochemistry, University of Notre Dame, Notre Dame, IN 46556, USA
e-mail: Danilo.H.JaraQuinteros.1@nd.edu

F. Guzman
Núcleo de Biotecnología Curauma, Pontificia Universidad Católica de Valparaíso, Avenida Universidad 330, Curauma, Valparaiso, Chile
e-mail: fanny.guzman@ucv.cl

I. O. Osorio-Roman (✉)
Department of Chemistry and Biochemistry, University of Windsor, Windsor, ON, Canada
e-mail: igor.orlando@gmail.com

dots not conjugated with the peptide. Moreover, the results show that the CLPFFD-functionalized nanoparticles bind to β-Amyloid fibres.

Keywords Cadmium telluride quantum dots · β-Amyloid fibres · Peptide CLPFFD · Cell viability

Introduction

In the last 20 years, nanotechnology has emerged as a technological answer to the new challenges derived from human development (Fadel et al. 2015; Huang et al. 2012; Let there be light 2015). Particularly, nanotechnological applications involving highly fluorescent semiconductor nanoparticles (NPs), or quantum dots (QD), have gained importance (Let there be light 2015). Because of their special spectroscopic properties and broad applications, cadmium telluride quantum dots (CdTe QD) are one of the most relevant semiconductor nanoparticles described to date and are being extensively used for producing solar cells, optoelectronic devices and biological applications (Bang and Kamat 2009; Díaz et al. 2012; Faraon et al. 2007; Kongkanand et al. 2008; Let there be light 2015; Ramirez-Maureira et al. 2015). When compared with organic fluorophores, QD exhibit important advantages; these include narrow emission spectra and "tuneable" spectroscopic properties due to the capability of QD to generate multi-colour fluorescence with a single excitation wavelength, high quantum yields and photochemical stability (Díaz et al. 2012; Erbo et al. 2008; Osovsky et al. 2007; Ramirez-Maureira et al. 2015). QD can be used for in vivo imaging applications via the multiphoton fluorescence technique (Larson et al. 2003). Although QD have interesting properties, they exhibit poor biocompatibility, which hinders their use in biological systems. Capping QD with biomolecules can improve QD biocompatibility (Díaz et al. 2012; Erbo et al. 2008; Lewinski et al. 2008; Lovrić et al. 2005; Pérez-Donoso et al. 2012).

In this context, aqueous synthesis of CdTe NPs capped with macromolecules or biomolecules (e.g. antibodies, receptor ligands, peptides, polymers) represents a strategy to promote their stability and biocompatibility. Some research groups are using peptides as capping agents for QD synthesis to improve the stability and properties (e.g. fluorescence) of the NPs while increasing biocompatibility (Díaz et al. 2012; Dumas et al. 2009; Erbo et al. 2008; Lewinski et al. 2008; Lovrić et al. 2005). Protocols for synthesizing glutathione (GSH)-capped CdTe QD (QD-GSH) have been described in our previous reports (Díaz et al. 2012; Ramirez-Maureira et al. 2015).

For the detection of toxic β-Amyloid protein (Aβ) aggregates involved in Alzheimer's disease, Tokuraku et al. conjugated $A\beta_{40}$ to QD to monitor the aggregation of Aβ in cells (Tokuraku et al. 2009), which is very interesting as an alternative method for the potential detection of this disease. However, it can be risky to use Aβ-functionalized QD as a system for in vivo diagnosis because undesired aggregation could occur in the brain and produce toxic effects. Instead, for the use of Aβ in this work, we conjugated the peptide LPFFD to the QD, which attaches selectively to Aβ and inhibits the formation of the toxic aggregates in the brain. As was demonstrated by Soto et al. (1996), the sequence LPFFD, which is a fragment corresponding to the physiological Aβ molecule (1–42), recognizes a particular (hydrophobic) domain of the β-sheet structure (the sequence ^{17}LVF^{20}F) and reduces Aβ toxicity in vivo (Soto et al. 1998). To functionalize the QD, we incorporated a Cys (C) residue at the extreme N-terminus of the peptide, which contains a thiol group that forms covalent bonds with Cd atoms on the surface of the QD (Díaz et al. 2012; Pérez-Donoso et al. 2012; Zhang et al. 2009). In addition, we demonstrated in a previous work that CLPFFD chemisorbs on the surface of gold nanoparticles and increases their stability (Olmedo et al. 2008).

To reduce the effects on cell viability, to increase the stability of CdTe QD coated with glutathione and to recognize Aβ aggregates, we conjugated QD with the peptide CLPFFD, resulting in the conjugate QD-GSH/CLPFFD. This paper focuses on the preparation and the spectroscopic characterization of the functionalized nanoparticles, and effects on cell viability and interaction with Aβ aggregates were studied.

Experimental

Synthesis of the CLPFFD peptide

The peptide, as a C-terminal amide, was obtained by solid-phase synthesis using an (Fmoc)/tert-butyl (tBu)

strategy. Cysteine side chains protected by the trityl groups were treated during the final cleavage to render the free thiols. The Fmoc-AM handle from Novabiochem (Laufelfingen, Switzerland) and the MBHA resin from Iris Biotech (Marktredwitz, Germany) were functionalized at a level of 0.7 mmol/g. The details of the synthesis protocol and HPLC methodology for the CLPFFD peptide have been previously described (Adura et al. 2013). The peptide was purified using semipreparative RP-HPLC with a waters 2487 dual absorbance detector equipped with a waters 2700 sample manager, a waters 600 controller, a waters fraction collector, a symmetry column (C18, 5 μm, 30 × 100 mm) and millennium software. The peptide was finally characterized through amino acid analysis with a Beckman 6300 analyser and through MALDI-TOF with a Bruker model Biflex III. Using MALDI-TOF, the CLPFFD (H-CLPFFD-NH_2) [M+ Na+]: 762.3 peptide was identified. The peptide was subjected to amino acid analysis, which yielded the following relationships, where the parentheses denote the theoretical relationship for CLPFFD: Leu 0.99 (1); Pro 1.06 (1); Phe 2.05 (2); Asp (0.90); and Cys not determined. HRMS calculated for $C_{36}H_{50}N_7O_8$ S [M+ H+], 740.3436; found, 740.3434. The purity determined by HPLC–UV was 95 %.

Synthesis of CdTe QD

Sodium borohydride (98 %), glutathione (GSH) (>98 %), sodium tetraborate, trisodium citrate, cadmium chloride and potassium tellurite were purchased from Sigma-Aldrich. Milli-Q grade water (>18 MΩ) was used as the solvent for aqueous solutions.

The synthesis of CdTe QD was performed based on the conditions described in a protocol developed by Ying et al. (Erbo et al. 2008), with some modifications (Díaz et al. 2012; Ramirez-Maureira et al. 2015). CdTe QD were synthesized with GSH as the capping agent. The synthesis of QD-GSH was carried out in 50 mL of a solution containing 15 mM $Na_2B_4O_7$ and 15 mM citrate buffer solution pH = 9.0. Then, $CdCl_2$, Na_2TeO_3 and $NaBH_4$ were added at 1, 0.25 and 20 mM final concentrations, respectively, and the solution was stirred vigorously for 5 min. Finally, 20 mM (final concentration) glutathione was added to the solution, which was then incubated at 90 °C for ~8 h after the solution reached a red colour. Collected samples were stored at 4 °C. Capped CdTe QD were precipitated with two volumes of ethanol and centrifuged for 3 min at 13,400×g. The supernatant was discarded, and purified QD were dissolved in buffer solution.

Quantum dot conjugation to peptide

A volume of 100 μL of QD-GSH (30 μg/mL) was mixed with 1 mL of CLPFFD peptide (1 mg/mL). The solution was incubated for 12 h at 4 °C and filtered using an Amicon Ultra-4 (3 kDa) microfilter to remove the excess unbound peptide. This procedure was performed three additional times until the peptide was not detected by a Micro BCA Protein Assay Kit (Pierce Biotechnology).

Characterization of quantum dots

Size and zeta potential of QD

The size of the QD-GSH and QD-GSH/CLPFFD was determined from images obtained using high-resolution transmission electron microscopy (HR-TEM), JEOL 2010; QD-GSH solutions were placed onto 400 mesh carbon-coated Cu grids. The average size of the QD was calculated using the sizes of 20 nanoparticles from five images (supplementary Figure S1). The hydrodynamic radius and the zeta potential of the QD-GSH and QD-GSH/CLPFFD were determined at 25, using DLS (dynamic light scattering) on a Zetasizer Nano-ZN. (Malvern Instruments Limited, UK), operating at a light source wavelength of 633 nm and with a fixed scattering angle of 175°. These measurements were performed in a cell with an optical path of 1 cm. To determine the size distribution of the samples, the results were analysed from the maximum intensity distribution values using the cumulants method. The electrophoretic determinations of zeta potential were made in aqueous media and a moderate electrolyte concentration. The Smoluchowski approximation was used to calculate zeta potential from the electrophoretic mobility measured. The average size and zeta potential were determined from three independent measurements for each QD solution.

Stability of QD

To evaluate the colloidal stability of the QD-GSH and QD-GSH/CLPFFD, both QD solutions were

centrifuged at 15,700×*g* for 15 min, and the QD were resuspended in water. Then, the hydrodynamic diameter of the QD-GSH and QD-GSH/CLPFFD were recorded at 25 °C, before and after that the samples were centrifugated, using DLS (dynamic light scattering) on a Zetasizer Nano-Z (Malvern Instruments Limited, UK). The average size were determined from three independent measurements for each QD solution.

Spectroscopic characterization of QD with and without CLPFFD

The synthesized QD-GSH and QD-GSH functionalized with CLPFFD were characterized using UV–VIS spectrophotometry, fluorometry, infrared spectroscopy and Raman spectroscopy. Absorption spectra were recorded using Lambda 25 UV/VIS spectrophotometers (Perkin Elmer) and fluorescence spectra were measured in 384 Nunc well fluorescence microliter plates using a multi-mode plate reader SynergyMx (BioTek Instruments, Inc). Measurements were with the same dilution for both nanoparticles. Furthermore, IR spectroscopy studies were performed for the free peptide and the peptide attached to the QD; 1 mg of peptide was analysed in KBr. The QD samples were lyophilized to obtain approximately 1 mg of a solid. This solid was characterized using NIR-FT spectroscopy (Perkin Elmer, USA). The Raman studies were performed for free peptides and peptides attached to the QD in the form of solid samples. Raman spectra were recorded with a micro Raman Renishaw 1000 spectrometer equipped with a Leica microscope and a CCD detector. The laser excitation lines used were 632.5 and 785 nm. The spectra were obtained using an optical magnification of 50x. The spectral resolution was 4 cm^{-1}, three accumulations were used and spectral scans of 30 s were registered. The Raman spectra were recorded in the 300–3500 cm^{-1} region. These spectral scanning conditions were chosen to avoid sample degradation.

Calculation of QD concentration

Cd and Te contents were determined using inductively coupled plasma (ICP) and an aliquot of known volume of QD-GSH/CLPFFD; 5 mL of QD was mixed with 5 mL of 5 M HNO_3 at 30 °C for 2 h to perform the digestion. The solution was then cooled and brought to a volume of 10 mL with distilled water in a volumetric flask; then, measurements were performed on the instrument. This procedure was repeated for three independent samples of QD-GSH/CLPFFD. The quantity of QD was estimated using the Cd^{2+} and Te^{2-} ions, assuming that each nanoparticle contained 80 % of Cd^{2+} and 20 % of Te^{2-}. Details of these calculations have been previously described by the authors and are provided in the supplementary materials (Ramirez-Maureira et al. 2015). With the Cd and Te concentration data and knowing the diameter of the CdTe QD (determined by HR-TEM), the concentration (nanomolar) of the QD was determined as follows. First, the spherical volume of a QD was calculated from the radius obtained by HR-TEM and using the following equation: $V = 4\pi r^3/3$. Then, the Cd^{2+} ion quantity for each QD was determined with this value, the atomic volume of Cd (5.4×10^{-3} nm^3), and taking into account that a Cd ion occupies 80 % of the volume of a QD. Finally, the QD concentration was calculated from the calculated number of Cd atoms for each nanoparticle and the concentration of this ion obtained by ICP. This calculation was also performed for Te, and both concentrations obtained were averaged.

Estimation of the number of peptide molecules per QD

The estimation of the number of peptide molecules per nanoparticle is necessary to determine the concentration of nanoparticles and the concentration of peptide in the same solution of functionalized QD. In one aliquot of the solution, the concentration of the nanoparticles was determined as described in the previous section. In another aliquot, the peptide concentration was determined by amino acid analysis. For this, 14 mL of QD-peptide solution (obtained from the synthesis) was lyophilized. The resulting solid was hydrolyzed for 72 h in 6 N HCl with a known quantity of amino butyric acid as an internal standard. Then, the solution was evaporated under reduced pressure and derivatized for the amino acid analysis by HPLC.

The number of peptide molecules per QD was calculated by dividing the number of peptide molecules per mL of solution by the number of QD particles per mL of solution.

Interactions between QD, Aβ fibres and oligomers

$A\beta_{1\text{-}42}$ (Yale University) was dissolved in water, aliquoted, lyophilized and stored in glass vials at −20 °C until use. The $A\beta_{1\text{-}42}$ aliquots were treated with 1,1,1,3,3,3-hexafluoro-2-propanol for 30 min to obtain the monomeric $A\beta_{1\text{-}42}$ form, and aliquots were then lyophilized and resuspended in PBS (phosphate-buffered saline) to obtain mature $A\beta_{1\text{-}42}$ fibres or soluble Aβ oligomers (AβOs).

Incorporation of QD into Aβ fibres

To determine whether the QD incorporate during the aggregation process into mature fibres, Aβ peptide solution (38 μM) with PBS was incubated with and without QD-GSH/CLPFFD for 48 h at 37 °C with mechanical stirring (350 rpm). In addition, to study the interaction with mature fibres, Aβ was first incubated for 48 h at 37 °C, and then the fibres were incubated for 1 h at 37 °C with mechanical stirring (300 rpm) with or without QD-GSH/CLPFFD (final concentration of nanoparticles 1.2×10^{14}/per ml).

To determine the loading of the Aβ fibres with QD-GSH/CLPFFD, the mature Aβ fibres bound to the QD (pellet) were separated from the unbound QD-GSH/CLPFFD (supernatant) by being centrifuged for 15 min at $2600\times g$. Then, the percent of unbound QD-GSH/CLPFFD in the supernatant was determined using fluorescence (as described previously). Moreover, the Aβ concentration in the supernatant was determined using a Micro BCA Protein Assay Kit (Pierce Biotechnology), which allowed us to calculate the ratio of Aβ fibres to QD-GSH/CLPFFD.

Interaction of QD with AβOs

To obtain soluble Aβ oligomers (AβOs), the peptide solution (0.38 mM) with PBS, was incubated overnight at 4 °C and was centrifuged for 10 min at $14{,}000\times g$ at 4 °C to remove insoluble fibres (Araya et al. 2008; Bieschke et al. 2008). Then, the supernatant containing soluble AβOs was incubated for 1 h at 4 °C with and without QD-GSH/CLPFFD with mechanical stirring.

In addition, Aβ fibres and AβOs incubated with or without QD-GSH/CLPFFD were observed using transmission electron microscopy (TEM). The samples were allowed to adsorb for 1 min to form colloidal films on glow-discharged, carbon-coated, 200 mesh copper grids. The TEM grids were then blotted and washed in Milli-Q water before being negatively stained with 1 % uranyl acetate for visualization by TEM (JEOL JEM-1010).

Cell viability assay

SH-SY5Y cells were maintained in low-glucose DMEM supplemented with 10 % inactivated foetal bovine serum (FBS), 2 mM glutamine, 50 U/mL penicillin and 0.05 g/mL streptomycin at 37 °C in a humidified atmosphere of 5 % CO_2.

To determine the effect of the QD-GSH functionalized with CLPFFD peptide on cell viability, the cells were seeded onto 96-well plates with low-glucose DMEM supplemented with 10 % FBS and were incubated overnight. The cells were treated with a series of concentrations of QD-GSH and QD-GSH/CLPFFD; 24 h later, cell viability was determined by a colorimetric end-point (490 nm) MTS assay according to the manufacturer's instructions (Promega). The absorbance of the QD at 490 nm in a blank was determined to evaluate potential interference in the MTS assay. For this purpose, the absorbance obtained with and without QD (10 μg/mL) was compared using the MTS assay under the same experimental conditions of the cell viability assay, but without cells. It was observed that the average absorbance values under the three conditions were not significantly different (supplementary Table S1); therefore, the presence of the QD at these concentrations did not affect the results of the assays performed.

Results and discussion

The conjugation of QD-GSH with CLPFFD led to the formation of QD-GSH/CLPFFD. Figure 1 summarizes the conjugation mechanism of the CLPFFD peptide on the QD. This peptide displaces the GSH molecules, resulting in a mixed layer of both peptides. As we demonstrated previously in gold nanoparticles, the Cys chemisorbed peptides can be replaced partially by other thiols (Guerrero et al. 2012). In addition, Wolcott et al. and Tansakul et al., have demonstrated the exchange of the QD surface functionalization. The authors agree that the surface of the QD has space for the addition of other capping agents

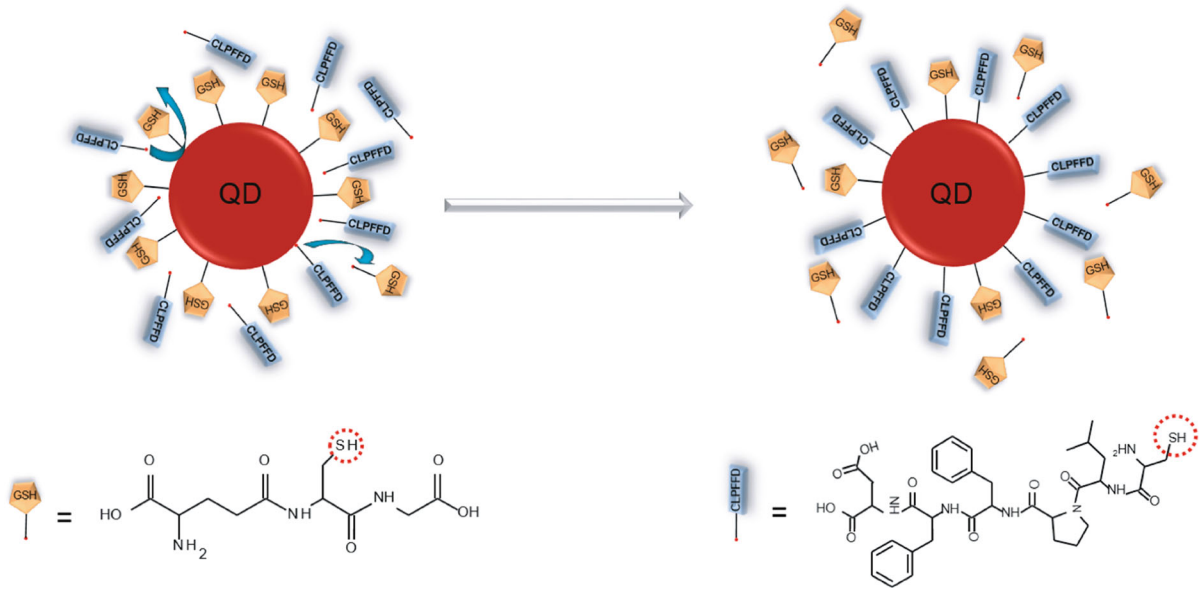

Fig. 1 Diagram of the conjugation QD-GSH with the CLPFFD peptide

(Califano 2015; Díaz et al. 2012; Hoshino et al. 2004; Kairdolf et al. 2013; Patra and Samanta 2014; Smith and Nie 2010).

The mean hydrodynamic diameters of the QD-GSH and QD-GSH/CLPFFD were 4.2 ± 0.3 and 6.5 ± 0.6 nm (Table 1), respectively. These results are in agreement with those obtained by HR-TEM (Fig. 2c, d, e). The size of the nanocrystal was calculated using the HR-TEM images (supplementary Figure S1) and was approximately 4.2 ± 0.3 nm. In addition, in Fig. 2d and e, it is possible to observe the crystalline structure of CdTe. The arrangement of the atoms shows a crystal face of the nanoparticle. The mean zeta potentials (Table 1) of the QD-GSH and QD-GSH/CLPFFD were similar (-26.1 ± 0.5 and -20.3 ± 0.7 mV, respectively), which can be attributed to the similar isoelectric point values, which were 5.9 and 5.6 for glutathione and CLPFFD, respectively.

Table 1 Characterization of QD-GSH and QD-GSH/CLPFFD

Nanoparticle	DLS (d.nm)	Z potential (mV)
QD-GSH	4.2 ± 0.3	-26.1 ± 0.5
QD-GSH/CLPFFD	6.5 ± 0.6	-20.3 ± 0.7

Dynamic light scattering (d. nm), Z potential (mV) and peptide number for QD. The results represent the mean and SEM, n = 3

The absorption spectrum for the QD-GSH was compared with that of the QD-GSH functionalized with CLPFFD peptide (Fig. 2a). For the QD-GSH, a characteristic absorbance at 530 nm was observed, and a blue shift close to 10 nm was observed after the functionalization of the QD-GSH with the CLPFFD. In the fluorescence spectra, the same blue shift was observed, with 590 nm corresponding to the QD-GSH and 580 nm corresponding to the QD-GSH/CLPFFD (Fig. 2b).

In both cases, the blue shifts are due to the addition of the peptide as a capping agent and the different surface charge values (Table 1). In this particular case, the capping agent changes the band gap, or electronic transition states, of the nanocrystal. This effect has been observed by other authors, and their results are in agreement with our results because these are characteristic properties of QD (Califano 2015; Díaz et al. 2012; Hoshino et al. 2004; Kairdolf et al. 2013; Patra and Samanta 2014; Smith and Nie 2010). In comparison with band gap changes of the more commonly studied CdSe, CdTe is softer and has a larger band gap deformation potential, which means that surface changes, such as adding a peptide, has an effect on the absorption and emission spectrum (Smith and Nie 2010).

To confirm the presence of CLPFFD in the CdTe QD, vibrational studies with FT-IR and Raman were

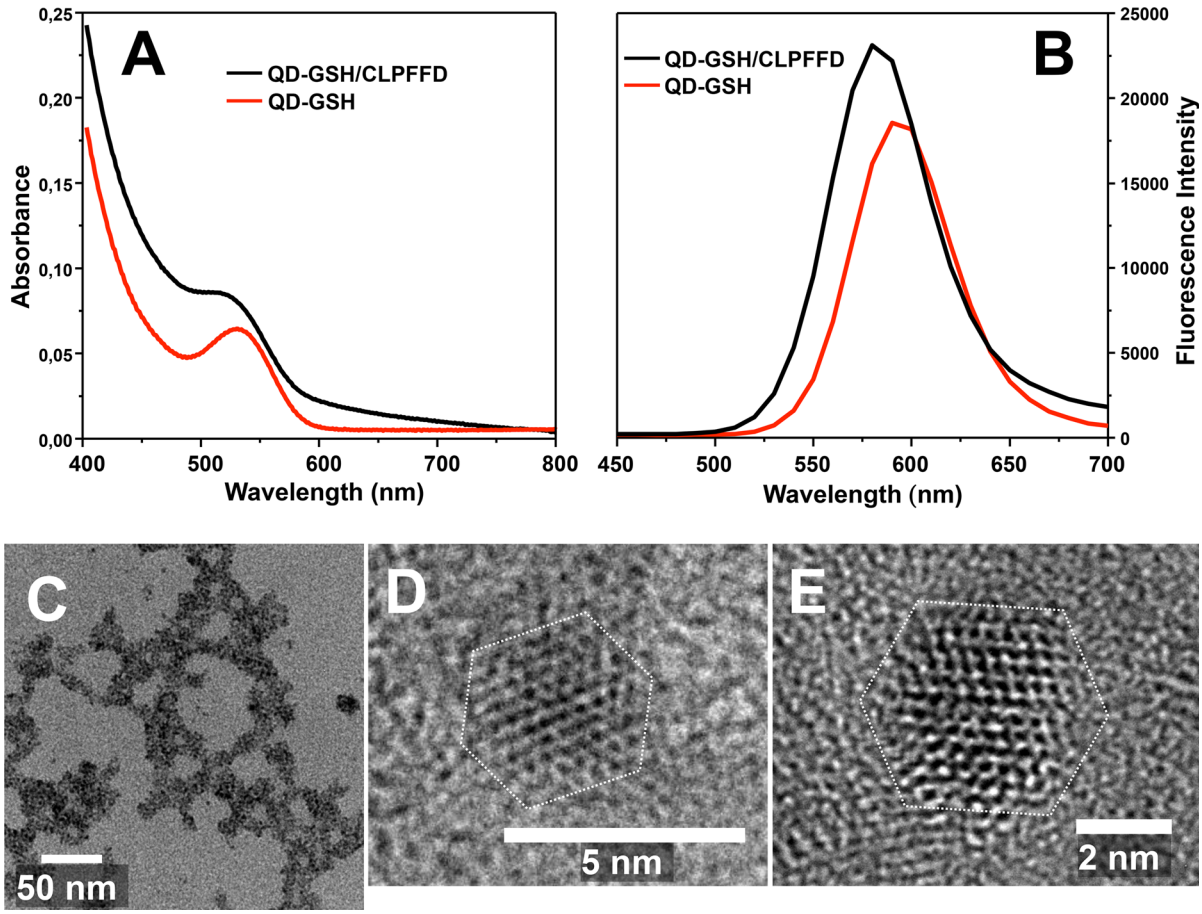

Fig. 2 Characterization of QD-GSH and QD-GSH/CLPFFD. On *top*, **a** and **b** show the absorption and fluorescence spectra, respectively, of QD-GSH (*red line*) and QD-GSH/CLPFFD (*black line*). Images **c**, **d** and **e** show high-resolution transmission electron microscopy (HR-TEM), on the scale of 50, 5 and 2 nm, respectively. The images **c** and **d** correspond to QD-GSH and image **e** correspond to QD-GSH/CLPFFD. (Color figure online)

conducted using CLPFFD as a standard (Fig. 3). The FT-IR spectrum of the peptide (Fig. 3a) showed the characteristic signals of amino acids: broad absorption bands at approximately 1670 cm^{-1} ($–COO^-$ group), 1455 cm^{-1} (antisymmetric $–COO^-$) and 1280 cm^{-1} (OH), indicating the presence of a –COOH group. Characteristic –N–H stretching modes observed at 3404 and 2960 cm^{-1} provided evidence of an $–NH_2$ group. The characteristic –SH stretching mode can be clearly observed at 2634 cm^{-1}. As expected, the IR absorption bands of the main functional groups, –COOH, $–NH_2$ and –SH, were detected in the CLPFFD control. In the QD-GSH/CLPFFD, the disappearance of the S–H group vibration at 2634 cm^{-1} was likely the result of covalent bond formation between the thiol and the Cd atom at the CdTe QD surface, suggesting the oxidation of cysteine residues (Fig. 3a in red). This covalent bond has been observed in previous studies with CdTe QD (Díaz et al. 2012; Pérez-Donoso et al. 2012; Zhang et al. 2009).

The Raman spectra of the peptide showed the characteristic signals of amino acids, corresponding with the FT-IR results. The most relevant vibrations are the following: 2940–2950 cm^{-1}, characteristic of –CH; bands near 1600, 1200 and 1000 cm^{-1}, corresponding to amide I, –CH and –NH deformations, and ring breathing, respectively; and bands near 620 cm^{-1}, corresponding to –CS stretching. (Stewart and Fredericks 1999; Vera et al. 2015) The characteristic –SH stretching mode at 2570 cm^{-1} (Fig. 3b) was very weak in the Raman spectra, but it was possible to observe, and we could see that the –SH stretching

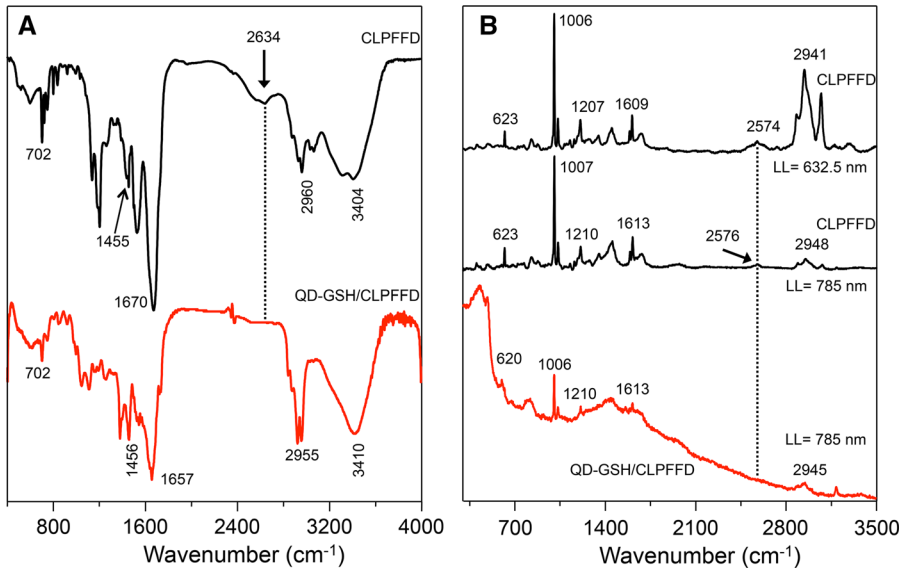

Fig. 3 **a** FT-IR spectra obtained from CLPFFD peptide (*black line*) and QD-GSH/CLPFFD (*red line*). **b** Raman spectra (*black line*) correspond to CLPFFD peptide using the 632 and 785 nm *laser line*. Raman spectrum (*red line*) corresponds to QD-GSH/CLPFFD using the 785 nm *laser line*. (Color figure online)

mode was not present in the QD-GSH/CLPFFD Raman spectra (Fig. 3b in red). In this sense, the Raman spectra reinforce the idea that the peptide is attached to the QD, and both spectroscopy methodologies (i.e. FT–IR and Raman) showed the same results that indicated the covalent attachment of CLPFFD to the QD-GSH.

The number of peptide molecules per QD-GSH/CLPFFD was 7 GSH and 95 CLPFFD molecules. Assuming that a QD has spherical shape and a diameter of 4.2 ± 0.3 nm, a surface area of 55.6 nm^2 is obtained. Each CLPFFD peptide molecule has an area of 0.6 nm^2; presuming a cylindrical conformation extending along the surface of the QD (with a cylindrical base), a maximum of 93 peptides per QD is expected. Therefore, it was concluded that the QD were mostly coated with CLPFFD, having almost completely displaced the tripeptide GSH from the surface of the QD.

To assess whether capping the QD with the CLPFFD peptide increases the colloidal stability, the QD-GSH and QD-GSH/CLPFFD were centrifuged at $15{,}700 \times g$ and resuspended in water; the hydrodynamic diameters were then determined. The results showed that the QD-GSH/CLPFFD were more stable than the QD-GSH. The QD-GSH/CLPFFD exhibited a slight increase in hydrodynamic diameter (8.5 ± 0.5 nm, pdI = 0.3), unlike the QD-GSH, which exhibited a 100-fold increase in hydrodynamic diameter (427 ± 95 nm, pdI = 1). These experiments demonstrate that coating QD-GSH with CLPFFD peptide increases stability with respect to QD-GSH.

In addition, the interaction between the QD-GSH/CLPFFD and Aβ fibres or AβOs was evaluated. First, we determined whether functionalized QD were incorporated during the assembly process or interacted with mature fibres. We incubated the QD-GSH/CLPFFD with AβOs for 48 h and, in parallel, we incubated the QD with formed fibres for 1 h. The samples were centrifuged, and the fluorescence of the supernatants was determined being similar in both cases. The intensity of the fluorescence signal corresponds to solutions of QDs with concentrations of 2.5×10^{13} and 2.4×10^{13} QD/mL, respectively, which indicates that approximately 80 % of the initial concentration of QDs interacts directly with formed fibres. However, the interaction of QDs can occur in later stages of the aggregation process from AβO to fibres resulting in a similar proportion of interaction between Aβ and nanoparticles. In relation with this, TEM results showed that the QD-GSH/CLPFFD interacted with the Aβ fibres (Fig. 4), but AβOs incubated with the QD-GSH/CLPFFD for 1 h at 4 °C showed no evidence of the nanoparticles binding to the AβOs (supplementary Figure S2). In accordance with this, last result is possible to consider that at least in the first stage of aggregation of Aβ process there is no interaction with QD-GSH/CLPFFD.

To determine the ratio of QD-GSH/CLPFFD interacting with Aβ fibres after incubation, the samples

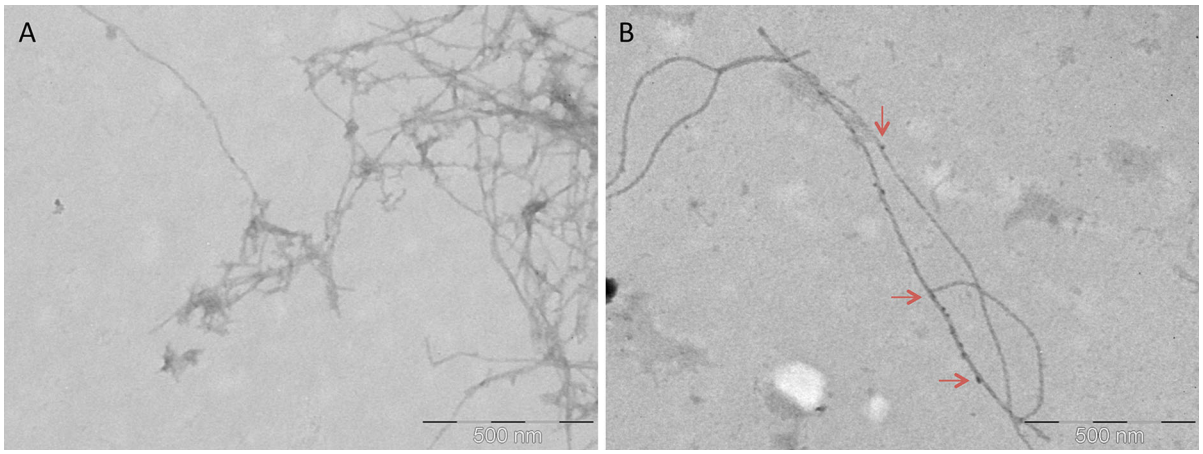

Fig. 4 Transmission electron microscopy (TEM) images. **a** Aβ fibres and **b** Aβ fibres with QD-GSH/CLPFFD that were incubated for 48 h. Image **b** shows the attachment of the QD-GSH/CLPFFD to the amyloid fibres (*red arrows*) on a scale of 500 nm. (Color figure online)

were centrifuged, and the concentrations of QD and Aβ in the supernatant were obtained. Taking into account that the difference between the total concentrations of QD and Aβ and the concentrations in the supernatant, it is possible to assume that the ratio Aβ/QD was: 5.8 nanomol Aβ to $9.6 \times 10^{13.}$ QDsGSH/CLPFFD nanoparticles (i.e. 1 nanoparticles per 36 molecules of Aβ). The QD-GSH/CLPFFD interacted with the amyloid fibres, as was previously demonstrated for gold nanoparticles conjugated with CLPFFD (Kogan et al. 2006; Olmedo et al. 2008). At the extreme C-terminus, the CLPFFD-NH_2 peptide contains an Asp residue (D) that confers primary amphipathicity to the molecule (i.e. in the C-terminal end of the sequence, there is a polar, charged residue, and in the rest of the sequence, there are predominantly hydrophobic residues), and increases the solubility of the peptide molecule. The presence of the Leu (L), Phe (F) and Phe (F) residues also present in the native sequence confers to the molecule the ability to recognize the Aβ aggregates (Soto et al. 1996) through interactions with the hydrophobic residues of the putative sequence ^{17}LVF^{20}F.

Additionally, the effect of the QD-GSH on the viability (with or without CLPFFD) of human neuroblastoma SH-SY5Y cells was evaluated using an MTS assay. The QD-GSH/CLPFFD affected cell viability to a lesser extent than did the QD-GSH (Fig. 5). Therefore, it can be concluded that the functionalization of QD with the CLPFFD peptide reduces the cytotoxic effects by 60 % at the highest dose tested (5 and 10 μg/mL) with respect to that of the cells treated with QD-GSH. This can be attributed to the CLPFFD peptide, which prevents the inorganic core of the QD from coming into contact with the cells, whereas the tripeptide GSH does not. Capping with GSH was not enough to reduce cell death (cytotoxicity was observed at 5 μg/mL). However, the QD capped with CLPFFD peptide exerted no detrimental effects on cell viability.

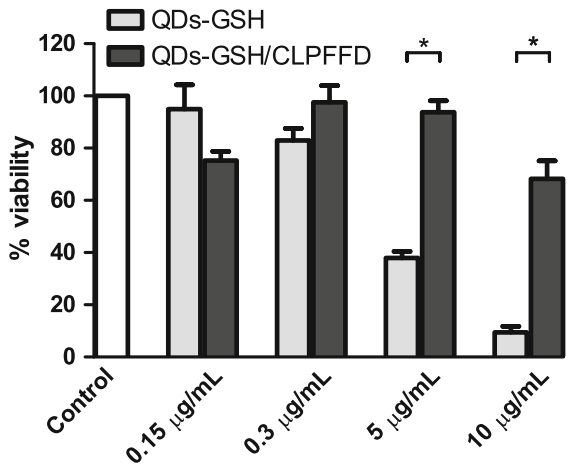

Fig. 5 Cell viability assay of QD-GSH and QD-GSH/CLPFFD in the SH-SY5Y cells. This cell were incubated with 0.15–10 μg/mL of QD-GSH and QD-GSH/CLPFFD for 24 h. The results are expressed as percentages compared with untreated cells (*white block*) and represent the mean and SEM, n = 4; statistical significance was evaluated by student's *t* test analysis *$p < 0.05$

The literature suggests that QD toxicity depends on multiple factors inherent to the physicochemical and environmental conditions. QD size, surface charge, concentration and capping agent, among other properties, play roles both collectively and individually in determining QD biocompatibility (Bradburne et al. 2013; Hardman 2006; Kuzyniak et al. 2014). The surface modification of QD and the changes in their physicochemical properties, such as solubility, are necessary not only to protect the QD core from oxidation and reduce toxicity by avoiding exposure of the Cd and Te atoms to the cellular environment but also to promote photoluminescent performance (Hardman 2006).

During the last 15 years, QD have been extensively used as biological markers and diagnostic tools (Bruchez et al. 1998; Chan and Nie 1998), being a better alternative to traditional fluorescent markers (Congo red and thioflavin-T) mainly due to high photosensitivity and the capacity to be used for drug delivery (Jameson et al. 2012; Medintz et al. 2005; Tokuraku et al. 2009). For such purposes, it is fundamental for this system to be able to cross the blood–brain barrier (BBB). In this context, Guerrero et al. (2010) demonstrated that when this CLPFFD peptide, which has amphipathic behaviour, was conjugated with gold nanoparticles, it promoted a major crossing of the gold nanoparticles through the BBB. Experiments with QD along this avenue of investigation are currently in progress in our laboratory.

Conclusion

In this study, a method of conjugated QD-GSH with CLPFFD peptide was developed. This method maintained the optical properties of the QD and generated nanoparticles with low cytotoxicity that were soluble in aqueous media and exhibited the capacity to interact with Aβ fibres.

The lower effects on cell viability of the QD-GSH/CLPFFD could be explained by the addition of a new stabilizer with more functional groups (i.e. the CLPFFD peptide), which allowed for more separation between the cells and the core of the nanoparticles, isolating the Cd and Te atoms from the biological environment and, therefore, enhancing cell viability with respect to that resulting from incubation with QD not capped with CLPFFD.

Therefore, it is believed that QD-GSH/CLPFFD can be a very useful tool for the early detection of amyloid aggregates, which is currently crucial for the early diagnosis of Alzheimer's disease. However, it is necessary to perform both ex vivo and in vivo experiments to probe the potential of the functionalized QD for clinical applications.

Acknowledgments Financial support of this paper was provided by the FONDECYT 3130654; Fondap 15130011 and FONDECYT 1130425 Grants.

References

Adura C et al (2013) Stable conjugates of peptides with gold nanorods for biomedical applications with reduced effects on cell viability. ACS Appl Mater Interfaces 5:4076–4085. doi:10.1021/am3028537

Araya E, Olmedo I, Bastus NG, Guerrero S, Puntes VF, Giralt E, Kogan MJ (2008) Gold Nanoparticles and microwave irradiation inhibit β-Amyloid amyloidogenesis. Nanoscale Res Lett 3:435–443. doi:10.1007/s11671-008-9178-5

Bang JH, Kamat PV (2009) Quantum dot sensitized solar cells. A tale of two semiconductor nanocrystals: CdSe and CdTe. ACS Nano 3:1467–1476. doi:10.1021/nn900324q

Bieschke J, Siegel SJ, Fu Y, Kelly JW (2008) Alzheimer's Aβ peptides containing an isostructural backbone mutation afford distinct aggregate morphologies but analogous cytotoxicity. Evidence for a common low-abundance toxic structure(s)? Biochemistry 47:50–59. doi:10.1021/bi701757v

Bradburne CE et al (2013) Cytotoxicity of quantum dots used for in vitro cellular labeling: role of qd surface ligand, delivery modality, cell type, and direct comparison to organic fluorophores. Bioconjug Chem 24:1570–1583. doi:10.1021/bc4001917

Bruchez M, Moronne M, Gin P, Weiss S, Alivisatos AP (1998) Semiconductor nanocrystals as fluorescent biological labels. Science 281:2013–2016. doi:10.1126/science.281.5385.2013

Califano M (2015) Origins of photoluminescence decay kinetics in CdTe colloidal quantum dots. ACS Nano 9:2960–2967. doi:10.1021/nn5070327

Chan WCW, Nie S (1998) Quantum dot bioconjugates for ultrasensitive nonisotopic detection. Science 281: 2016–2018. doi:10.1126/science.281.5385.2016

Díaz V et al (2012) Spectroscopic properties and biocompatibility studies of cdte quantum dots capped with biological thiols. Sci Adv Mater 4:609–618

Dumas EM, Ozenne V, Mielke RE, Nadeau JL (2009) Toxicity of CdTe quantum dots in bacterial strains. IEEE Trans Nanobiosci 8:56–64

Erbo Y, Dan L, Shaojun G, Shaojun D, Jin W (2008) Synthesis and bio-imaging application of highly luminescent mercaptosuccinic acid-coated CdTe nanocrystals. PLoS One 3:e2222–e2227

Fadel TR, Steevens JA, Thomas TA, Linkov I (2015) The challenges of nanotechnology risk management. Nano Today 10:6–10. doi:10.1016/j.nantod.2014.09.008

Faraon A, Englund D, Fushman I, Vučković J, Stoltz N, Petroff P (2007) Local quantum dot tuning on photonic crystal chips. Appl Phys Lett 90:213110. doi:10.1063/1.2742789

Guerrero S et al (2010) Improving the brain delivery of gold nanoparticles by conjugation with an amphipathic peptide. Nanomedicine 5:897–913. doi:10.2217/nnm.10.74

Guerrero S et al (2012) Synthesis and in vivo evaluation of the biodistribution of a 18F-labeled conjugate gold-nanoparticle-peptide with potential biomedical application. Bioconjug Chem 23:399–408. doi:10.1021/bc200362a

Hardman R (2006) A toxicologic review of quantum dots: toxicity depends on physicochemical and environmental factors. Environ Health Perspect 114:165–172. doi:10.1289/ehp.8284

Hoshino A et al (2004) Physicochemical properties and cellular toxicity of nanocrystal quantum dots depend on their surface modification. Nano Lett 4:2163–2169. doi:10.1021/nl048715d

Huang Y-Y et al. (2012) Can nanotechnology potentiate photodynamic therapy? vol 1. doi:10.1515/ntrev-2011-0005

Jameson LP, Smith NW, Dzyuba SV (2012) Dye-binding assays for evaluation of the effects of small molecule inhibitors on amyloid (Aβ) self-assembly. ACS Chem Neurosci 3:807–819. doi:10.1021/cn300076x

Kairdolf BA, Smith AM, Stokes TH, Wang MD, Young AN, Nie S (2013) Semiconductor quantum dots for bioimaging and biodiagnostic applications. Ann Rev Anal Chem 6:143–162. doi:10.1146/annurev-anchem-060908-155136

Kogan MJ et al (2006) Nanoparticle-mediated local and remote manipulation of protein aggregation. Nano Lett 6:110–115. doi:10.1021/nl0516862

Kongkanand A, Tvrdy K, Takechi K, Kuno M, Kamat PV (2008) Quantum dot solar cells. Tuning photoresponse through size and shape control of CdSe–TiO2 architecture. J Am Chem Soc 130:4007–4015. doi:10.1021/ja0782706

Kuzyniak W et al (2014) Synthesis and characterization of quantum dots designed for biomedical use. Int J Pharm 466:382–389. doi:10.1016/j.ijpharm.2014.03.037

Larson DR, Zipfel WR, Williams RM, Clark SW, Bruchez MP, Wise FW, Webb WW (2003) Water-soluble quantum dots for multiphoton fluorescence imaging in vivo. Science 300:1434–1436. doi:10.1126/science.1083780

Let there be light (2015) Nat Mater 14:453. doi:10.1038/nmat4287

Lewinski N, Colvin V, Drezek R (2008) Cytotoxicity of nanoparticles. Small 4:26–49

Lovrić J, Bazzi HS, Cuie Y, Fortin GRA, Winnik FM, Maysinger D (2005) Differences in subcellular distribution and toxicity of green and red emitting CdTe quantum dots. J Mol Med 83:377–385

Medintz IL, Uyeda HT, Goldman ER, Mattoussi H (2005) Quantum dot bioconjugates for imaging, labelling and sensing. Nat Mater 4:435–446

Olmedo I et al (2008) How changes in the sequence of the peptide CLPFFD-NH2 can modify the conjugation and stability of gold nanoparticles and their affinity for β-amyloid fibrils. Bioconjug Chem 19:1154–1163. doi:10.1021/bc800016y

Osovsky R, Kloper V, Kolny-Olesiak J, Sashchiuk A, Efrat Lifshitz E (2007) Optical Properties of CdTe nanocrystal quantum dots, grown in the presence of Cd^0 nanoparticles. J Physic Chem C 111:10841–10847

Patra S, Samanta A (2014) Effect of capping agent and medium on light-induced variation of the luminescence properties of CdTe quantum dots: a study based on fluorescence correlation spectroscopy, steady state and time-resolved fluorescence techniques. J Physic Chem C 118:18187–18196. doi:10.1021/jp5048216

Pérez-Donoso JM et al (2012) Biomimetic. Mild chemical synthesis of cdte-gsh quantum dots with improved biocompatibility PLoS One 7:e30741–e30749

Ramirez-Maureira M, Vargas V, Riveros A, Goulet PJG, Osorio-Román IO (2015) Shell-isolated nanoparticle-enhanced fluorescence (SHINEF) of CdTe quantum dots. Mater Chem Phys 2:351–356

Smith AM, Nie S (2010) Semiconductor Nanocrystals: structure, properties, and band gap engineering. Acc Chem Res 43:190–200. doi:10.1021/ar9001069

Soto C, Kindy MS, Baumann M, Frangione B (1996) Inhibition of alzheimer's amyloidosis by peptides that prevent β-sheet conformation. Biochem Biophys Res Commun 226:672–680. doi:10.1006/bbrc.1996.1413

Soto C, Sigurdsson EM, Morelli L, Asok Kumar R, Castano EM, Frangione B (1998) [beta]-sheet breaker peptides inhibit fibrillogenesis in a rat brain model of amyloidosis: implications for Alzheimer's therapy. Nat Med 4:822–826

Stewart S, Fredericks PM (1999) Surface-enhanced Raman spectroscopy of peptides and proteins adsorbed on an electrochemically prepared silver surface. Spectrochim Acta Part A Mol Biomol Spectrosc 55:1615–1640. doi:10.1016/S1386-1425(98)00293-5

Tokuraku K, Marquardt M, Ikezu T (2009) Real-time imaging and quantification of amyloid-β peptide aggregates by novel quantum-dot nanoprobes. PLoS One 4:e8492. doi:10.1371/journal.pone.0008492

Vera AM, Cárcamo JJ, Aliaga AE, Gómez-Jeria JS, Kogan MJ, Campos-Vallette MM (2015) Interaction of the CLPFFD peptide with gold nanospheres. A Raman, surface enhanced Raman scattering and theoretical study. Spectrochimica Acta Part A: Mol Biomol Spectrosc 134:251–256. doi:10.1016/j.saa.2014.06.116

Zhang L, Xu C, Li B (2009) Simple and sensitive detection method for chromium (VI) in water using glutathione-capped CdTe quantum dots as fluorescent probes. Microchim Acta 166:61–68